Cellular and Molecular Biology
E-ISSN : 1165-158X / P-ISSN : 0145-5680
www.cellmolbiol.org

Identification of biomarkers associated with oxidative stress-related genes in postmenopausal osteoporosis

Dan Liu, Zhijun Hu*, Zhanying Tang, Pan Li, Weina Yuan, Fangfang Li, Qian Chen

Department of Rehabilitation Medicine, Longhua Hospital Affiliated to Shanghai University of Traditional Chinese Medicine, Shanghai, China

ARTICLE INFO

Original paper

Article history:
Received: February 08, 2023
Accepted: June 18, 2023
Published: June 30, 2023

Keywords:

postmenopausal osteoporosis, oxidative stress-related genes, WGCNA, signature genes, TF-miRNA-mRNA network

ABSTRACT

Osteoporosis (OP) is a prevalent metabolic disease, with aging and menopause being the major risk factors. Studies have shown that nearly one-third of postmenopausal women suffer from osteoporosis. However, there is a scarcity of research on antioxidant systems for the prevention and treatment of postmenopausal osteoporosis (PM-OP). To address this gap, we performed differential analysis using Limma to identify differentially expressed genes (DEGs) in PM-OP samples. We employed weighted correlation network analysis (WGCNA) to identify oxidative stress (OS)-related genes (OSRGs) highly correlated with PM-OP. The intersection of key modular genes and DEGs yielded differentially expressed OSRGs (DE-OSRGs) specific to PM-OP. We conducted GO and KEGG functional enrichment analyses on these genes. Additionally, we constructed a protein-protein interaction (PPI) network and utilized support vector machine recursive feature elimination (SVM-RFE) and random forest (RF) algorithms to identify signature genes. The diagnostic value of the signature genes was evaluated and validated using ROC curves. GSEA enrichment analysis was employed to explore the potential mechanisms associated with the signature genes. Finally, we constructed a regulatory network involving TF-miRNA-mRNA interactions for the signature genes and verified the biological roles of FOXO3 and DDIT3 in PM-OP and healthy groups using quantitative real-time PCR (qRT-PCR). Our analysis revealed 20 DE-OSRGs specific to PM-OP, obtained by intersecting modular and differential genes. The PPI network identified central genes (DDIT3, MAPK8, CDK2, SIRT1, and FOXO3) with more than 3 nodes. Through integration with machine learning algorithms, we identified DDIT3 and FOXO3 as signature genes. The ROC curve analysis indicated that the AUC value was greater than 0.7, suggesting the potential diagnostic value of these signature genes. Furthermore, GSEA results revealed their involvement in pathways related to the regulation of neutrophil activation, oxidative phosphorylation, MAPK signaling, mitochondrial matrix, and phagocytosis. Lastly, we constructed a regulatory network comprising 27 nodes (22 TFs, 3 miRNAs, and 2 mRNAs) and 28 edges. Additionally, qRT-PCR confirmed the significant up-regulation of FOXO3 and DDIT3 expressions in the PM-OP group compared to the healthy control group. In summary, this study employed bioinformatics analysis to identify OS-related biomarkers (DDIT3 and FOXO3) in PM-OP, providing new biological targets for clinical treatment.

Doi: http://dx.doi.org/10.14715/cmb/2023.69.6.28

Introduction

Osteoporosis (OP), induced as the imbalance of bone remodeling, is a kind of chronic bone disease with the typical clinical manifestation of pain, limited limb movement, muscle weakness and bone fracture (1). In 2019, an estimated 25.5 million women and 6.5 million men lived with osteoporosis in the EU, Switzerland and the UK, and the population of males and females over 50 is expected to increase by 11.4% between 2019 and 2034, and the number of osteoporotic fractures per year in these countries will increase by 25% (2). The National Osteoporosis Foundation estimates that 10.2 million Americans have osteoporosis and another 43.4 million will have low bone mass by 2021, and the population with OP or low bone mass will probably reach 71 million by 2030 (3, 4). OP poses a huge threat to public health worldwide (5-7). Postmenopausal osteoporosis (PM-OP) refers to the presence of OP in postmenopausal women, which is related to the decline of ovarian function and subsequent downregulated estrogen levels (8, 9). PM-OP is characterized by bone resorption over bone formation, low bone mass and deterioration of the skeletal microarchitecture, which contribute to the increased susceptibility to fragility fractures, thus leading to disability and mortality worldwide (10). Bone tissue development, differentiation, bone mineralization and bone resorption are dynamic metabolic processes, which are mainly regulated by osteoblasts and osteoclasts (11, 12). The imbalance of bone formation and bone resorption triggers the progression of PM-OP, among which endocrine and metabolic factors play a crucial role with age (13, 14).

Among all metabolic-related factors, oxidative stress (OS) is one of the most important factors during PM-OP (15, 16). OS is an oxidation reaction caused by oxygen free radicals and peroxides (17), and reactive oxygen species

* Corresponding author. Email: hzjz1062@163.com

(ROS) is the main cause of oxidative stress. Under physiological conditions, ROS maintains at a very low level and plays a role in signal transduction, secretion of inflammatory factors and cell apoptosis (18, 19). Current studies have shown that variations of oxidative stress markers such as superoxide dismutase (SOD), 2,2-diphenyl-1-picrylhydrazyl (DPPH) and ROS interact with osteoblasts, osteoclasts, fibroblasts, adipose tissue cells, and vascular endothelial cells to participate in the occurrence and development of PM-OP(20). For instance, SOD and DPPH are regarded as bone metabolic activity index, which could be used to evaluate and diagnose OP (21, 22). An increased SOD is symbolized a relative health condition of the bone, while the DPPH decline is a predictor of the dysfunction of bone metabolism. In the absence of estrogen protection, overloaded ROS breaks the balance between osteoblast and osteoclast, and promotes osteoblast apoptosis by inducing the mitochondrial apoptosis pathway (23). Besides, excessive ROS can induce osteoclast differentiation by activating MAPK, PI3K and NF-κB pathways (24). Although oxidative stress-related biomarkers are important for the prevention and treatment of PM-OP, few relevant studies have been reported.

In this light, bioinformatics analysis was performed to analyze differentially expressed genes (DEGs) and related-function enrichment in PM-OP patients and healthy populations in this study. Our data represented that bone metabolism is firmly related to the formation or regulation of oxidants, and two typical DEGs including DDIT3 and FOXO3 in PM-OP were identified. This study provides a molecular perspective for understanding the mechanism and developing a personalized treatment for patients with PM-OP.

Materials and Methods

Data sources

The transcriptome data of PM-OP and control peripheral blood samples were downloaded from the GEO database (https://www.ncbi.nlm.nih.gov/geo/), including the GSE56815 dataset (20 controls samples and 20 PM-OP samples) and GSE62402 dataset (5 control samples and 5 PM-OP samples). 1399 OSRGs were extracted from the GeneCards database (25).

DEGs analysis

The limma package (version 3.46.0) (26) was used to compare the differences in gene expression levels between control and PM-OP samples in the GSE56815 dataset. The differential gene screening conditions were as follows: $|\log_2 FC| > 0.5$, P-value < 0.05. The volcano map and heat map were plotted with ggplot2 (version 3.3.6) and pheatmap (version 1.0.12), respectively.

Weighted gene co-expression network analysis

The R software package WGCNA (version 1.71) (27) was used to analyze OSRGs with similar expression patterns and to search for modular genes that were highly correlated with OP. Firstly, the samples were clustered to see if outliers need to be removed, and the appropriate soft threshold was selected based on the near-scale-free topological criteria. The OSRGs were divided into different modules by dynamic cutting method. Then, the correlation of different modules with the disease or control was calculated and the module with the highest correlation with PM-OP was selected as the key module. The genes in the key modules were defined as OSRGs associated with PM-PO.

Functional enrichment analysis

DEGs and key module genes were intersected to obtain differentially expressed OSRGs (DE-OSRGs) in PM-OP. Then, ClusterProfiler (version 3.18.1) (28) was used for GO and KEGG functional enrichment analysis for these genes.

Building protein-protein interaction (PPI) network

The STRING database was used to obtain protein interaction information, which was used to create a PPI network for DE-OSRGs.

SVM-RFE and RF machine learning

DE-OSRGs were analyzed using SVM-RFE and RF (29) machine-learning algorithms to narrow down the range of signature genes. And the genes obtained by the PPI network, SVM-RFE and RF were intersected to obtain the signature genes (or biomarkers).

Receiver operating characteristic (ROC) analysis

ROC curves were drawn by the pROC package (version 2.3.0) (30) to evaluate the diagnostic value of biomarkers. The larger the area under the curve (AUC), the higher the accuracy.

Gene set enrichment analysis (GSEA)

Single-gene gene set enrichment analysis (GSEA) (31) analysis was performed to find the significant pathways of signature genes. The filtering criteria were |NES| > 1, P. adjust < 0.05 and q values < 0.25.

TF-miRNA-mRNA network construction

The transcription factors (TF)-mRNA relationship pairs of signature genes were extracted from the TRRUST database, and the Sankey map was drawn using "ggalluvial" (version 0.12.3) package for visualization. The upstream miRNAs of the signature genes were predicted by Mirwalk, TargetScan and miRTarBase databases, respectively, and the intersection result was the predicted miRNA. Sankey plots were drawn for visualization. Finally, TF-mRNA and miRNA-mRNA relationship pairs were merged and visualized using Cytoscape software (version 3.7.1) (32).

Research object and sample collection

A total of 10 patients with clinically confirmed postmenopausal osteoporosis were selected to collect clinical data, and 10 normal subjects were used as controls. The fasting blood of all subjects was collected in the morning. 8 mL venous blood of each patient was taken and allowed to stand for 30 min, and the upper serum (non-hemolytic state) was collected by centrifugation at 4°C 3000 g/min for 10 min, and centrifuged at 13500 g/min for 4 min at 4°C. The serum was split into Eppendorf (EP) tubes with 200 uL per tube and placed in a -80°C refrigerator for storage. This study was approved by the Ethics Committee of Longhua Hospital Affiliated to the Shanghai University of Traditional Chinese Medicine. Signed written informed consent were obtained from all participants.

Table 1. The sequences of primers.

Name	Primer
FOXO3-Forward	5'-CGGACAAACGGCTCACTCT-3'
FOXO3-Reverse	5'-GGACCCGCATGAATCGACTAT-3'
DDIT3-Forward	5' -GGAAACAGAGTGGTCATTCCC-3'
DDIT3-Reverse	5'-CTGCTTGAGCCGTTCATTCTC-3'
β-actin-Forward	5'-CATGTACGTTGCTATCCAGGC-3'
β-actin-Reverse	5'-CTCCTTAATGTCACGCACGAT-3'

Quantitative real-time polymerase chain reaction (qRT-PCR)

The total RNA from serum was isolated using TRIzol reagent (Invitrogen, Carlsbad, CA, USA). RNA purity was measured on a Nucleic acid protein quantifier (DS-11, Denovix, USA). Then RNA was transcribed into complementary deoxyribose nucleic acid (cDNA) using the Hi-FiScript gDNA removal cDNA synthesis kit (CW2582M, Cwbio, Beijing, China) followed by analysis using qRT-PCR with the SYBR Mixture (MQ00401S, Monad, China) based on the expression of β-actin on a CFX Connect™ Real-Time PCR System (Bio-Rad, Hercules, CA, USA) to collect and analyze the data. The primers applied for the qRT-PCR reaction are shown in Table 1.

Statistical analysis

All bioinformatics analyses were undertaken in R language. The Wilcoxon test was employed to contrast the data from different groups. Statistical comparisons were performed using GraphPad Prism (v 8.0, La Jolla, CA, USA), and the comparisons between the two groups were performed with independent samples t-test or Mann-Whitney test dependent on whether the data conforms to the Gaussian distribution. P-values <0.05 were considered statistically significant.

Results

Screening of DE-OSRGs in PM-OP

Firstly, the difference in gene expression levels between PM-OP and control samples was compared. A total of 323 DEGs were obtained, among which 192 DEGs were up-regulated and 131 DEGs were down-regulated in PM-OP (Figure 1A-B). Then, WGCNA analysis was performed to find the OSRGs associated with OP. The sample clustering result indicated that there were no outliers (Figure 1C). 5 was the first value above 0.9, which could be considered as the soft threshold (Figure 1D). Next, the differences among genes were used to cluster the obtained topological matrix. The adjacency and similarity coefficients between genes were calculated to obtain different modules (Figure 1E). Then, the correlation between different modules and control or PM-OP was calculated. The MEblue had the highest correlation with the PM-OP (correlation value: 0.49, P = 0.001), which contained a total of 339 genes (Figure 1F-G). Finally, 20 DE-OSRGs in PM-OP were obtained by the intersection of DEGs and MEblue module genes (Figure 1H).

Functional enrichment of DE-OSRGs in PM-OP

To further explore the function involved in DE-OSRGs, GO and KEGG functional enrichment was conducted. 103 biological processes were mainly enriched, such as regulation of autophagy, response to nutrient levels, cellular response to reactive oxygen species, and positive regulation of response to endoplasmic reticulum stress (Figure 2A). Then, the DE-OSRGs were also involved in 25 pathways, such as the FOXO signaling pathway and Cellular senescence (Figure 2B).

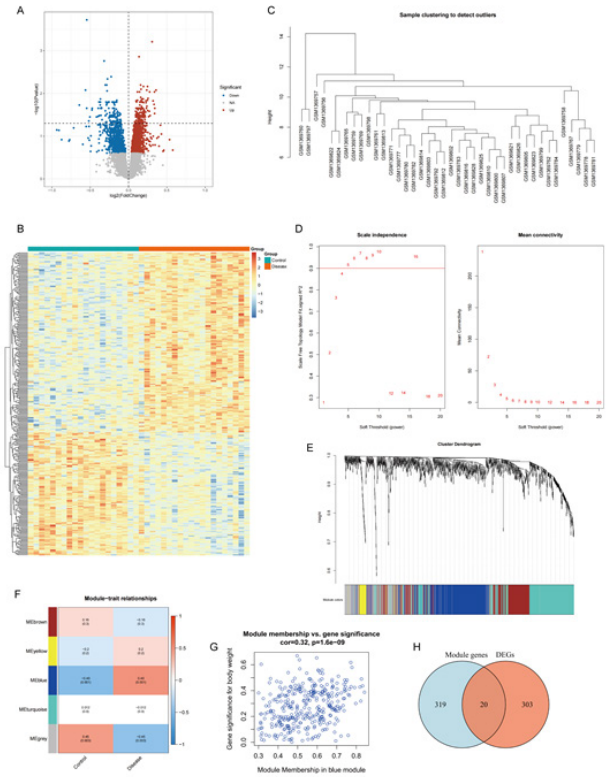

Figure 1. Screening of DE-OSRGs in PM-OP. Volcano plot (A) and heatmap (B) of DEGs. (C) Sample clustering to detect outliers. (D) Soft threshold analysis. (E) Adjacency and similarity coefficients between genes. (F) Module-trait relationships between control and disease. (G) Module membership vs. gene significance. (H) The intersection of DEGs and MEblue module genes is shown by the Venn diagram.

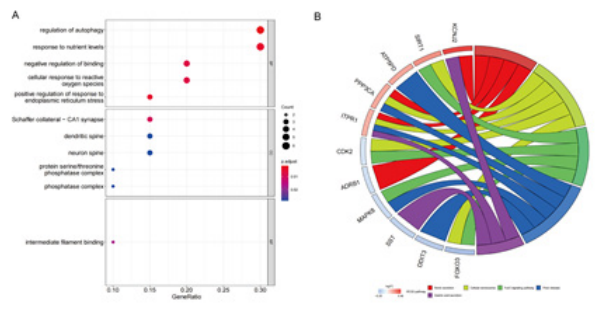

Figure 2. Functional enrichment of DE-OSRGs in PM-OP. A. GO analysis of DE-OSRGs. B. Pathways involved in DE-OSRGs.

Mining for signature genes

The STRING database was used to obtain protein interaction information, and the PPI network (which contains 11 nodes and 20 edges) was constructed for DE-OSRGs (Figure 3A). The PPI network was sorted by the number of nodes and genes with more than three nodes were selected, including DDIT3, MAPK8, CDK2, SIRT1 and FOXO3 (Figure 3B). Next, 6 genes were obtained by SVM-RFE screening based on DE-OSRGs (Figure 3C). Meanwhile, 11 genes were obtained by the RF algorithm (Figure 3D). Then, the genes obtained by PPI network analysis, SVM-RFE and RF algorithms were intersected to obtain signature genes (DDIT3 and FOXO3) (Figure 3E). The relative expression profiles of signature genes in all patients were exhibited in Figure 3F.

Evaluation of diagnostic efficiency of signature genes

Firstly, the ROC curve of signature genes was drawn to evaluate the diagnostic efficiency. The AUC area of DDIT3 was 0.805 and that of FOXO3 was 0.867, indicating that the diagnosis had a certain accuracy (Figure 4A). Secondly, verification was carried out in the GSE62402 dataset (Figure 4B). The AUC area of DDIT3 was 0.84 and that of FOXO3 was 0.72, indicating a certain diagnosis accuracy in the validation set.

Single-gene GSEA of DDIT3 and FOXO3

In order to understand the biological function and the involved signaling pathways of biomarkers, GSEA was performed. A total of 587 GO items (granulocyte activation, neutrophil activation and neutrophil mediated immunity, etc.) and 30 KEGG pathways (Aldosterone synthesis and secretion, Oxidative phosphorylation and Protein digestion and absorption, etc.) of DDIT3 were accessed (Figure 5A-B). GO enrichment of FOXO3 resulted in 12

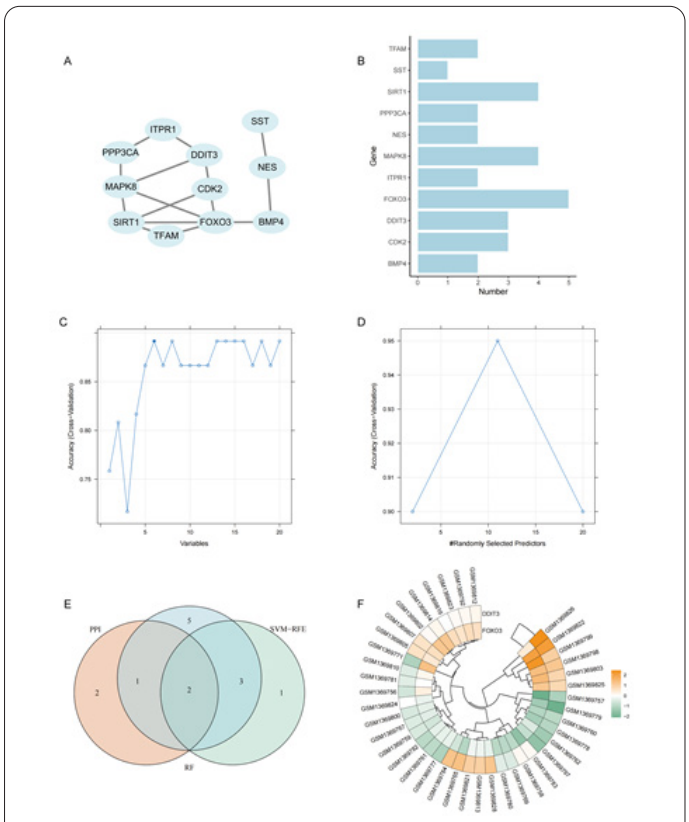

Figure 3. Signature genes mining. (A-B) PPI network constructed for DE-OSRGs. (C) SVM-RFE screening. (D) RF algorithm. (E) Intersected signature genes including DDIT3 and FOXO3. (F) Relative expression profiles of signature genes.

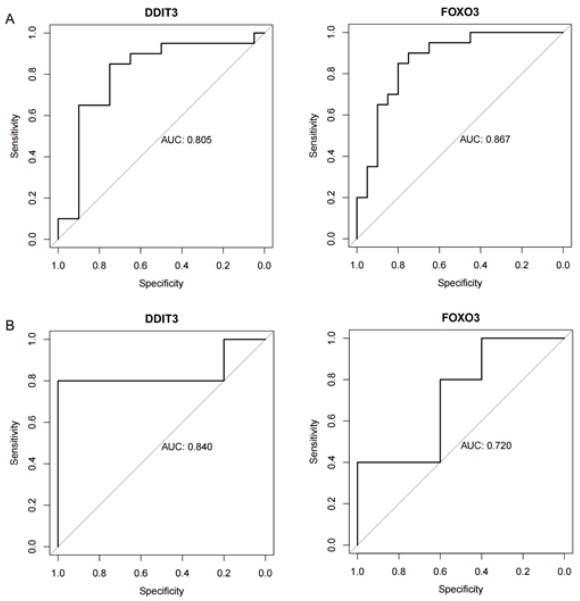

Figure 4. Diagnostic efficiency of signature genes. (A) The AUC area of DDIT3 and FOXO3. (B) Verification in GSE62402 dataset.

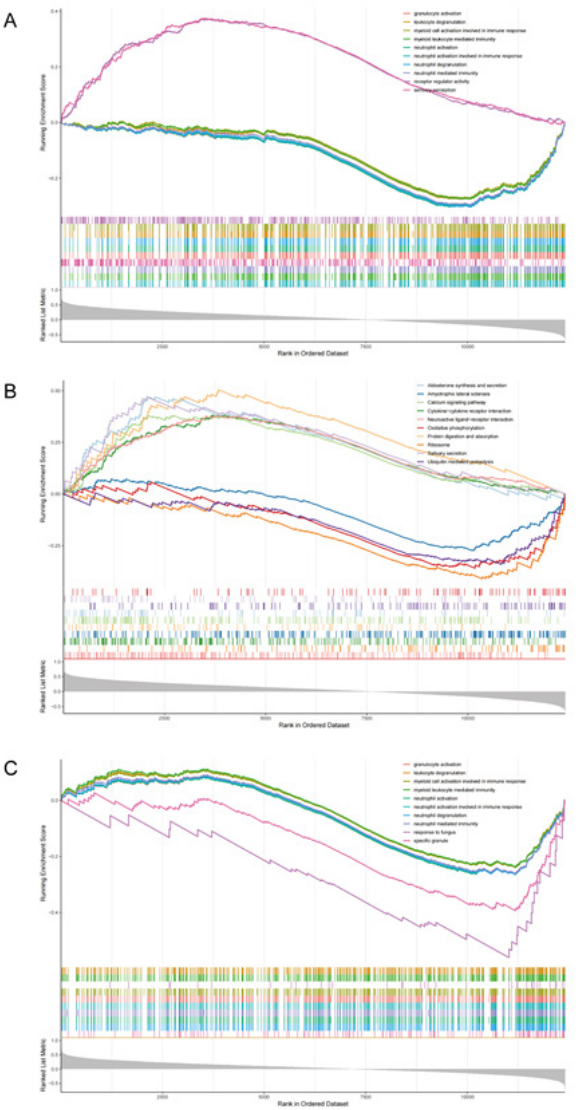

Figure 5. Single-gene GSEA of DDIT3 and FOXO3. 587 GO items (A) and 30 KEGG pathways (B) of DDIT3. (C) GO enrichment of FOXO3.

items (granulocyte activation, neutrophil degranulation and neutrophil mediated immunity, etc.) (Figure 5C). The figures showed the TOP 10 GO entries and KEGG pathways (Figure 5).

TF-miRNA-mRNA network construction

Firstly, 24 relationship pairs of TF-mRNA were identified according to DDIT3 and FOXO3 (Figure 6A). 3 intersected miRNAs were predicted from different databases (Figure 6B), and the miRNA-mRNA regulatory relationship diagram was established based on the 3 miRNAs and 2 signature genes (Figure 6C). Finally, the TF-mRNA and miRNA-mRNA relationship pairs were merged to construct the TF-miRNA-mRNA regulatory relationship network, containing 27 nodes (specifically 22 TF, 3 miRNA and 2 mRNA) and 28 edges (Figure 6D), in which RB1, RBCA1 and JDP2, etc. regulated DDIT3, RELA, ABL1 and NFKB1, etc. regulated FOXO3, hsa-miR-96-5p regulated DDIT3 and FOXO3, hsa-miR-9-5p and hsa-miR-29a-3p regulated FOXO3.

Biological verification of FOXO3 and DDIT3 in postmenopausal osteoporosis patients

The biological roles of FOXO3 and DDIT3 in PM-OP and healthy groups were verified by qRT-PCR. Our results showed that FOXO3 and DDIT3 expressions were both significantly up-regulated in the PM-OP group compared with the healthy control group (all $P<0.05$) (Figure 7), indicating a consistent alternative tendency with the results of bioinformatic analysis.

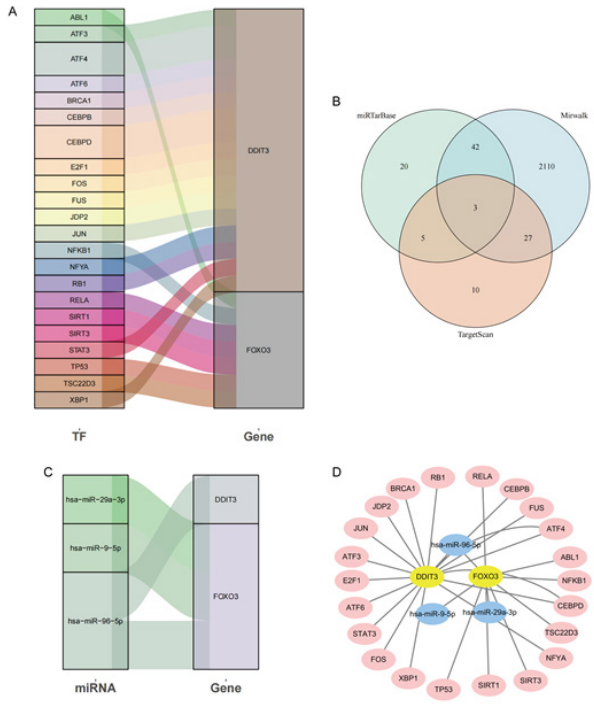

Figure 6. TF-miRNA-mRNA network of DDIT3 and FOXO3. (A) 24 relationship pairs of TF-mRNA based on DDIT3 and FOXO3. (B) 3 intersected miRNAs from different databases. (C) miRNA-mRNA regulatory relationship diagram. (D) TF-miRNA-mRNA regulatory relationship network.

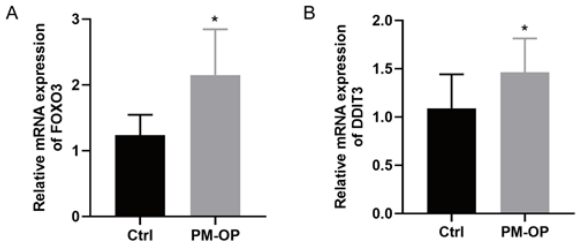

Figure 7. The expressions of FOXO3 and DDIT3 in Postmenopausal Osteoporosis Patients The RNA expressions of FOXO3 (A) and DDIT3 (B) in Postmenopausal Osteoporosis Patients were detected by qRT-PCR. $P<0.05$.

Discussion

OP is well-identified that several factors contribute to its occurrence and progression, and menopause is one of the leading causes of OP in the female population(33). Besides, the abnormal oxidative stress level has been considered a key regulator in the balance of osteoblasts and osteoclasts (34). However, few studies about oxidative stress-related biomarkers in PM-OP have been reported till now. Our study explored OS-related biomarkers such as DDIT3 and FOXO3 through bioinformatics analysis in PM-OP, offering novel molecular targets for the clinical treatment of PM-OP.

The imbalance of OS has been widely implicated in the occurrence and progression of PM-OP. A recent meta-analysis reported by Zhao et al. (15) indicated that oxidative stress index and advanced oxidation protein products were significantly increased in PM-OP patients, whereas the total antioxidant status, total antioxidant power, catalase and glutathione peroxidase were decreased. Besides, it has been confirmed that dietary pyrroloquinoline quinone, a natural antioxidant, could inhibit osteoclastic bone resorption and enhance osteoblastic bone formation by suppressing oxidative stress, thus preventing ovariectomy-induced bone loss and improving bone strength (35). In line with our results, we also noticed the presence of an association between bone metabolism and oxidant regulation, with the oxidative signaling pathways involved in osteoblast differentiation and apoptosis. Further, KEGG enrichment analysis identified six oxidative stress-related pathways including mitochondrial biosynthesis, DNA damage repair, histone acetylation modification, Wnt/β-catenin signaling pathway and cytoskeletal regulation. Similarly, Yang et al. (36) glutathione/oxidized glutathione (GSH/GSSG) conversion involved the PI3K/Akt-Nrf2/HO-1 signaling pathway and that the antioxidant enzyme-mediated mitochondrial apoptosis pathway of osteoblasts was necessary for the development of PM-OP.

We subsequently performed PPI analysis and identified intersecting signature genes including DDIT3 and FOXO3. The following ROC curve and AUC area validated the relatively high diagnostic efficiency of these two signature genes in this study. Moreover, the qRT-PCR was further performed to verify the alternations of DDIT3 and FOXO3, and the results represented that FOXO3 and DDIT3 were both significantly increased in the PM-OP group compared with the healthy control group. DDIT3 has been reported to play a role in impeding osteoblast mineralization and promoting apoptosis (37). Here, 587 GO items (granulocyte activation, neutrophil activation and neutrophil mediated immunity, etc.) and 30 KEGG pathways (Aldosterone synthesis and secretion, Oxidative phosphorylation and Protein digestion and absorp-

tion, etc.) of DDIT3 were screened out, suggesting that the DDIT3 may regulate PM-OP progression via OS and innate immune-relevant pathways. Another signature gene FOXO3 is also involved in the regulation of oxidative stress-induced autophagy in bone cells, including osteoblasts, osteocytes and osteoclasts (38). In this study, GO enrichment of FOXO3 represented the contribution of granulocyte activation, neutrophil degranulation and neutrophil-mediated immunity. Zou et al. (39) reported that OS could induce apoptosis in OP through FOXO3a ubiquitylation and degradation. Therefore, we underscored the important roles of signature genes DDIT3 and FOXO3 in the development of PM-OP patients, which may contribute to the imbalance of bone remodeling through regulating OS.

MiRNA can perform post-transcriptional regulation by sequentially targeted binding to mRNA. Meanwhile, miRNA expression is also mediated by TF, thus forming a complex upstream and downstream regulatory network of miRNA, namely TF-miRNA-mRNA (40, 41). TF-miRNA-mRNA could help correlate the interaction of transcription factors, miRNA and target genes together, and visualize a network map, thus exploring potential key molecules more intuitively and conveniently (42, 43). In this study, the TF-miRNA-mRNA network construction results identified that RB1, RBCA1 and JDP2 regulated DDIT3, besides, RELA, ABL1 and NFKB1 regulated FOXO3. Moreover, hsa-miR-96-5p regulated DDIT3 and FOXO3, and hsa-miR-9-5p and hsa-miR-29a-3p regulated FOXO3. Till now, the potential role of miRNA in PM-OP remains elusive, we have identified the signature genes including DDIT3 and FOXO3, and constructed the signature genes-related TF-miRNA-mRNA network associated with signature genes. This may largely help further investigation on molecular mechanisms and serve as potential biomarkers or therapeutic targets for PM-OP.

Altogether, our study identified two OS-related biomarkers including DDIT3 and FOXO3 in patients with PM-OP by bioinformatics analysis. The prognostic value of DDIT3 and FOXO3 in PM-OP patients was firmly validated. Further signature genes-related pathways and TF-miRNA-mRNA were explored to elucidate the underlying molecular mechanisms in PM-OP. The specific mechanism is not fully elucidated in the present study, therefore, further studies about the mechanism of DDIT3 and FOXO3, and the larger clinical trials are worthy of performing in our future work.

Funding Acknowledgements

This work was supported by the National Key R&D Plan (NO: 2019YFC1709905); The three-year action plan for Shanghai to further accelerate the inheritance, innovation and development of traditional Chinese medicine (ZY (2021-2023) -0201-01); Pudong Famous Traditional Chinese Medicine Training Plan of Pudong New District Health System (PWRzm2020-15); 2022 Emergency Scientific Research and Tackling Project of Shanghai University of Traditional Chinese Medicine in Response to novel coronavirus Infection Pneumonia in Omicron (2022YJ-48); Artificial Intelligence Medical Hospital Local Cooperation Project of Xuhui District (2021-016).

Conflict of Interests

The authors declared no conflict of interest.

References

1. Kanis JA, Cooper C, Rizzoli R, Reginster JY. European guidance for the diagnosis and management of osteoporosis in postmenopausal women. Osteoporosis Int 2019; 30(1): 3-44.
2. Oniszczuk A, Kaczmarek A, Kaczmarek M, et al. Sclerostin as a biomarker of physical exercise in osteoporosis: A narrative review. Front Endocrinol 2022; 13: 954895.
3. Wright NC, Looker AC, Saag KG, et al. The recent prevalence of osteoporosis and low bone mass in the United States based on bone mineral density at the femoral neck or lumbar spine. J Bone Miner Res 2014; 29(11): 2520-2526.
4. Arceo-Mendoza RM, Camacho PM. Postmenopausal Osteoporosis: Latest Guidelines. Endocrin Metab Clin 2021; 50(2): 167-178.
5. Clynes MA, Harvey NC, Curtis EM, Fuggle NR, Dennison EM, Cooper C. The epidemiology of osteoporosis. Brit Med Bull 2020; 133(1): 105-117.
6. Salari N, Ghasemi H, Mohammadi L, et al. The global prevalence of osteoporosis in the world: a comprehensive systematic review and meta-analysis. J Orthop Surg Res 2021; 16(1): 609.
7. Wang L, Yu W, Yin X, et al. Prevalence of Osteoporosis and Fracture in China: The China Osteoporosis Prevalence Study. Jama Netw Open 2021; 4(8): e2121106.
8. Yong EL, Logan S. Menopausal osteoporosis: screening, prevention and treatment. Singap Med J 2021; 62(4): 159-166.
9. Vadaye KE, Fazly BB, Kerachian MA. Implantation of stem cells on synthetic or biological scaffolds: an overview of bone regeneration. Biotechnol Genet Eng 2021; 37(2): 238-268.
10. Polyzos SA, Anastasilakis AD, Efstathiadou ZA, Yavropoulou MP, Makras P. Postmenopausal osteoporosis coexisting with other metabolic diseases: Treatment considerations. Maturitas 2021; 147: 19-25.
11. Ballhause TM, Jiang S, Baranowsky A, et al. Relevance of Notch Signaling for Bone Metabolism and Regeneration. Int J Mol Sci 2021; 22(3): 1325.
12. Kaur M, Nagpal M, Singh M. Osteoblast-n-Osteoclast: Making Headway to Osteoporosis Treatment. Curr Drug Targets 2020; 21(16): 1640-1651.
13. Li L, Wang Z. Ovarian Aging and Osteoporosis. Adv Exp Med Biol 2018; 1086: 199-215.
14. Thapa S, Nandy A, Rendina-Ruedy E. Endocrinal metabolic regulation on the skeletal system in post-menopausal women. Front Physiol 2022; 13: 1052429.
15. Zhao F, Guo L, Wang X, Zhang Y. Correlation of oxidative stress-related biomarkers with postmenopausal osteoporosis: a systematic review and meta-analysis. Arch Osteoporos 2021; 16(1): 4.
16. Shahriarpour Z, Nasrabadi B, Hejri-Zarifi S, et al. Oxidative balance score and risk of osteoporosis among postmenopausal Iranian women. Arch Osteoporos 2021; 16(1): 43.
17. Forman HJ, Zhang H. Targeting oxidative stress in disease: promise and limitations of antioxidant therapy. Nat Rev Drug Discov 2021; 20(9): 689-709.
18. Hussain T, Tan B, Yin Y, Blachier F, Tossou MC, Rahu N. Oxidative Stress and Inflammation: What Polyphenols Can Do for Us? Oxid Med Cell Longev 2016; 2016: 7432797.
19. Su LJ, Zhang JH, Gomez H, et al. Reactive Oxygen Species-Induced Lipid Peroxidation in Apoptosis, Autophagy, and Ferroptosis. Oxid Med Cell Longev 2019; 2019: 5080843.
20. He Y, Wuertz-Kozak K, Kuehl LK, Wippert PM. Extracellular Vesicles: Potential Mediators of Psychosocial Stress Contribution to Osteoporosis? Int J Mol Sci 2021; 22(11): 5846.
21. Tan Y, Li X, Zhang Q, Zhou X, Zhang J. Surgical strategy and outcomes for thoracolumbar disc herniation with Autologous Bone-Fusion or Cage-Fusion surgery: case series and literature review.

Biotechnol Genet Eng 2022: 1-13.
22. El-Makawy AI, Ibrahim FM, Mabrouk DM, Abdel-Aziem SH, Sharaf HA, Ramadan MF. Efficiency of turnip bioactive lipids in treating osteoporosis through activation of Osterix and suppression of Cathepsin K and TNF-alpha signaling in rats. Environ Sci Pollut R 2020; 27(17): 20950-20961.
23. Sun JY, Hou YJ, Fu XY, et al. Selenium-Containing Protein From Selenium-Enriched Spirulina platensis Attenuates Cisplatin-Induced Apoptosis in MC3T3-E1 Mouse Preosteoblast by Inhibiting Mitochondrial Dysfunction and ROS-Mediated Oxidative Damage. Front Physiol 2018; 9: 1907.
24. Xiao L, Zhong M, Huang Y, et al. Puerarin alleviates osteoporosis in the ovariectomy-induced mice by suppressing osteoclastogenesis via inhibition of TRAF6/ROS-dependent MAPK/NF-kappaB signaling pathways. Aging (Albany NY) 2020; 12(21): 21706-21729.
25. Wu Z, Wang L, Wen Z, Yao J. Integrated analysis identifies oxidative stress genes associated with progression and prognosis in gastric cancer. Sci Rep-Uk 2021; 11(1): 3292.
26. Cai W, Li H, Zhang Y, Han G. Identification of key biomarkers and immune infiltration in the synovial tissue of osteoarthritis by bioinformatics analysis. Peerj 2020; 8: e8390.
27. Chen S, Yang D, Liu Z, et al. Crucial Gene Identification in Carotid Atherosclerosis Based on Peripheral Blood Mononuclear Cell (PBMC) Data by Weighted (Gene) Correlation Network Analysis (WGCNA). Med Sci Monitor 2020; 26: e921692.
28. Yu G, Wang LG, Han Y, He QY. clusterProfiler: an R package for comparing biological themes among gene clusters. Omics 2012; 16(5): 284-287.
29. Tang H, Han Q, Yin Y. Screening of Important Markers in Peripheral Blood Mononuclear Cells to Predict Female Osteoporosis Risk Using LASSO Regression Algorithm and SVM Method. Evol Bioinform 2022; 18: 1041331130.
30. Robin X, Turck N, Hainard A, et al. pROC: an open-source package for R and S+ to analyze and compare ROC curves. Bmc Bioinformatics 2011; 12: 77.
31. Xiao Y, Najeeb RM, Ma D, Yang K, Zhong Q, Liu Q. Upregulation of CENPM promotes hepatocarcinogenesis through mutiple mechanisms. J Exp Clin Canc Res 2019; 38(1): 458.
32. Dong Q, Han Z, Tian L. Identification of Serum Exosome-Derived circRNA-miRNA-TF-mRNA Regulatory Network in Postmenopausal Osteoporosis Using Bioinformatics Analysis and Validation in Peripheral Blood-Derived Mononuclear Cells. Front Endocrinol 2022; 13: 899503.
33. Black DM, Rosen CJ. Clinical Practice. Postmenopausal Osteoporosis. New Engl J Med 2016; 374(3): 254-262.
34. Massaccesi L, Galliera E, Pellegrini A, Banfi G, Corsi RM. Osteomyelitis, Oxidative Stress and Related Biomarkers. Antioxidants-Basel 2022; 11(6): 1061.
35. Geng Q, Gao H, Yang R, Guo K, Miao D. Pyrroloquinoline Quinone Prevents Estrogen Deficiency-Induced Osteoporosis by Inhibiting Oxidative Stress and Osteocyte Senescence. Int J Biol Sci 2019; 15(1): 58-68.
36. Yang K, Cao F, Xue Y, Tao L, Zhu Y. Three Classes of Antioxidant Defense Systems and the Development of Postmenopausal Osteoporosis. Front Physiol 2022; 13: 840293.
37. Li H, Li D, Ma Z, et al. Defective autophagy in osteoblasts induces endoplasmic reticulum stress and causes remarkable bone loss. Autophagy 2018; 14(10): 1726-1741.
38. Zhu C, Shen S, Zhang S, Huang M, Zhang L, Chen X. Autophagy in Bone Remodeling: A Regulator of Oxidative Stress. Front Endocrinol 2022; 13: 898634.
39. Zou DB, Mou Z, Wu W, Liu H. TRIM33 protects osteoblasts from oxidative stress-induced apoptosis in osteoporosis by inhibiting FOXO3a ubiquitylation and degradation. Aging Cell 2021; 20(7): e13367.
40. Fu Z, Xu Y, Chen Y, Lv H, Chen G, Chen Y. Construction of miRNA-mRNA-TF Regulatory Network for Diagnosis of Gastric Cancer. Biomed Res Int 2021; 2021: 9121478.
41. Ye Z, Fang J, Wang Z, et al. Bioinformatics-based analysis of the lncRNA-miRNA-mRNA and TF regulatory networks reveals functional genes in esophageal squamous cell carcinoma. Bioscience Rep 2020; 40(8): BSR20201727.
42. Luo X, Lu W, Zhao J, et al. Identification of the TF-miRNA-mRNA co-regulatory networks involved in sepsis. Funct Integr Genomic 2022; 22(4): 481-489.
43. Ke P, Qian L, Zhou Y, et al. Identification of hub genes and transcription factor-miRNA-mRNA pathways in mice and human renal ischemia-reperfusion injury. Peerj 2021; 9: e12375.